

# The interplay between neutral exciton and charge transfer states in single-strand polyadenine. A quantum dynamical investigation

## Supporting Information

Fabrizio Santoro,<sup>1,\*</sup> Roberto Improta,<sup>2\*</sup> Francisco Avila,<sup>1,3</sup> Mireia Segado,<sup>4</sup> and Alessandro Lami<sup>1</sup>

1) CNR--Consiglio Nazionale delle Ricerche, Istituto di Chimica dei Composti Organo Metallici (ICCOM-CNR), UOS di Pisa, Area della Ricerca, via G. Moruzzi 1, I-56124 Pisa, Italy

2) CNR--Consiglio Nazionale delle Ricerche, Istituto di Biostrutture Biommagini (IBB-CNR) Via Mezzocannone 16, I-80136, Napoli, Italy.

3) University of Málaga, Physical Chemistry, Faculty of Science, Málaga, 29071, Spain

4) INSTM UdR Pisa, c/o Dipartimento di Chimica e Chimica Industriale dell'Università di Pisa, Via Risorgimento 35, I-56126 Pisa, Italy

\*) Authors to whom correspondence should be addressed.

e-mail: [fabrizio.santoro@iccom.cnr.it](mailto:fabrizio.santoro@iccom.cnr.it), [robimp@unina.it](mailto:robimp@unina.it)

## S1.Methods

### S1.1 Vibronic Hamiltonian

The transition between exciton and CT states is accompanied by remarkable rearrangements of the nuclear structure. As anticipated in the main text, in order to describe the effect of the vibrational

motion on the time-evolution of the electronic populations we proposed [R. Improta et al J. Phys. Chem. A, 2009, 113, 15346–15354] a vibronic Hamiltonian, associating to each electronic state an harmonic potential energy surface (PES) .

$$H_{\text{vib}} = H_{\text{el}} + \sum_{i,j} |i, j\rangle \langle i, j| \left[ \sum_{v,\alpha} \left[ \frac{1}{2} \omega_v (Q_{v,\alpha} - Q_{v,\alpha}^0(ij))^2 - \frac{1}{2} \omega_v \frac{\partial^2}{\partial Q_{v\alpha}^2} \right] \right] \quad (3)$$

In Eq. 3 the coordinates  $Q_{k\alpha}$  are orthogonal combinations of the ground state normal modes of each unit where the first index (latin) identifies the vibration, while the second one (greek) indicates the unit where it is localized, the Hamiltonian is written in dimensionless coordinates and we neglect the effect of inter-units vibrations. We assume that the PESs share the same set of normal modes and frequencies (also with the ground state), while in general each state has a different equilibrium position  $Q_{k\alpha}^0(ij)$  (the couple of indexes in parenthesis specifies the electronic state).

As described in ref. [R. Improta et al J. Phys. Chem. A, 2009, 113, 15346–15354], the PESs associated to the involved diabatic states  $|j, k\rangle$  can be easily built on the ground of the PESs of the ground, cationic, anionic and excited states ( $A, A^+, A^-, A^*$ , respectively) of each unit. Despite the impressive progresses in modern methods for time-propagation of wave packets, like those based on multiconfigurational expansions [H. Beck et al Phys. Rep., 2000, 324, 1-105; 46) Multidimensional Quantum Dynamics. MCTDH Theory and Applications, ed. H.-D. Meyer, F. Gatti, and G. A. Worth, Wiley VCH, Weinheim, 2009], at the state of the art is still extremely challenging to compute the quantum dynamics of a medium-size (dozens of normal modes) system including all the nuclear degrees of freedom. Hierarchical representation of the Hamiltonians [E. Gindensperger et al, J. Chem. Phys., 2006, 124, 144103-144120; L. Cederbaum et al. Phys. Rev. Lett., 2005, 94, 113003-113006; D. Péicconi et al. J. Chem. Phys., 2012, 136, 244104-244120] allow to define few effective vibrational modes that describe accurately the short-time dynamics of

the system and represent a very promising technique to treat large-systems, most of all when coupled with more approximate (e. g. classical) descriptions of the motion along the less-important coordinates of the hierarchy. The effective modes of the first (most important) block of the hierarchy comprises the coordinates that describe the displacement from the ground state geometry to the minima of the different coupled PESs.

In ref. [R. Improta et al J. Phys. Chem. A, 2009, 113, 15346–15354] we adopted a similar recipe to define a minimal set of effective coordinates for the  $A_2$  dimer (in practice we considered the same coordinates arising from the hierarchical transformation, after neglecting normal modes with very low-frequency, since they are expected to move more slowly. In this way we selected three coordinates on each unit of Ade, that are the ones that physically describe the displacement from the minimum of the ground state  $A$ , to the minima of the cation, anion and neutral excited states  $A^+$ ,  $A^-$ ,  $A^*$ .

### **S1.2 Diabatic and adiabatic representation of the relaxation superoperator.**

We can describe our system adopting two different basis sets, the diabatic states  $|b_n\rangle = |j, k\rangle$  and the adiabatic states  $|a_n\rangle$  of the eigenstates of the Hamiltonian in Eq.1 in the main text. The two sets are connected by an orthogonal transformation so that, saying  $|\mathbf{b}\rangle_R$  and  $|\mathbf{a}\rangle_R$  the row vectors of the diabatic basis sets we have  $|\mathbf{a}\rangle_R = |\mathbf{b}\rangle_R \mathbf{C}$ . The density operator can be written (since now on we drop the “el” subscript) alternatively in the two basis sets ( $\mathbf{C}$  real)

$$\rho = |\mathbf{b}\rangle_R \boldsymbol{\rho}^b \langle \mathbf{b}|_C = |\mathbf{a}\rangle_R \mathbf{C}^T \boldsymbol{\rho} \mathbf{C} \langle \mathbf{a}|_R = |\mathbf{a}\rangle_R \boldsymbol{\rho}^a \langle \mathbf{a}|_R. \quad (\text{S1})$$

Where the subscript  $C$  indicates a vector column. It is useful at this point to switch to a superoperator notation  $|mn\rangle\rangle = |b_m\rangle\langle b_n|$  defining the scalar product as  $\langle\langle mn||rs\rangle\rangle = \text{Tr}[|b_n\rangle\langle b_m|b_r\rangle\langle b_s|]$ . The same can be done in the adiabatic basis set  $|\mu\nu\rangle\rangle = |a_\mu\rangle\langle a_\nu|$ , and  $\langle\langle\mu\nu||\sigma\tau\rangle\rangle = \text{Tr}[|a_\nu\rangle\langle a_\mu|a_\sigma\rangle\langle a_\tau|]$ . We then have

$$|\mu\nu\rangle\rangle = \sum_{mn} C_{m\mu} C_{n\nu} |mn\rangle\rangle \quad (\text{S2})$$

which in matrix form becomes (four indices are needed)

$$|\mu\nu\rangle\rangle = \sum_{mn} D_{\mu\nu;mn} |mn\rangle\rangle \quad \text{or} \quad |\mathbf{aa}\rangle\rangle_R = |\mathbf{bb}\rangle\rangle_R \mathbf{D} \quad (\text{S3})$$

In this representation the  $\rho$  operator is written as a linear combination of the basis set of operators  $|mn\rangle\rangle$ . In matrix form these reads  $\rho = |\mathbf{bb}\rangle\rangle_R \boldsymbol{\rho}_C^{bb} = |\mathbf{aa}\rangle\rangle_R \boldsymbol{\rho}_C^{aa}$ , where we simply sorted the operators  $|b_m b_n\rangle\rangle$  ( $|a_m a_n\rangle\rangle$ ) in a row vector and  $\boldsymbol{\rho}_C^{bb}$  ( $\boldsymbol{\rho}_C^{aa}$ ) are the column vectors of the coefficients (i.e. the elements of  $\boldsymbol{\rho}^b$  and  $\boldsymbol{\rho}^a$  respectively).

In a superoperator formalism  $\Gamma$  can be expressed like a four-indices matrix  $\Gamma_{mn;rs}$  so that  $\Gamma\rho = \mathbf{\Gamma}^b \boldsymbol{\rho}_C^{bb} = \mathbf{\Gamma}^a \boldsymbol{\rho}_C^{aa}$ . We might choose to insert a dephasing on the off-diagonal density-matrix elements either in the diabatic or in eingestates sets. The matrix elements in the two representations are respectively  $\Gamma_{mn;rs}^b = \langle\langle mn|\Gamma|rs\rangle\rangle$  and  $\Gamma_{\mu\nu;\sigma\tau}^a = \langle\langle\mu\nu|\Gamma|\sigma\tau\rangle\rangle$ . To avoid proliferation of parameters we attach the same dephasing time constant  $\tau_{deph}$  to any couple of states. Therefore, in formulas, the two possible choices for the dephasing (among diabatic or adiabatic states) are equivalent to set either  $\Gamma_{mn;rs}^b = \delta_{mr}\delta_{ns}(1-\delta_{rs})\tau_{deph}^{-1}$  or  $\Gamma_{\mu\nu;\sigma\tau}^a = \delta_{\mu\sigma}\delta_{\nu\tau}(1-\delta_{\mu\nu})\tau_{deph}^{-1}$ . At this point  $\Gamma$  in the other representation can be simply obtained by the relation  $\mathbf{\Gamma}^b = \mathbf{D}\mathbf{\Gamma}^a\mathbf{D}^T$  ( $\mathbf{D}$  real).

### S1.3 Dependence of the long-time limit of the populations on the choice to introduce a dephasing among diabatic or adiabatic states

The two options have a significantly different impact on the dynamics. This can be appreciated considering the case  $\tau_{A^*} = \infty$  (no decay of excitons) and computing the long-time limit of the populations (diagonal elements of the density matrix), when the coherences (non diagonal matrix elements) have been erased by dephasing (we work now in a generic representation and then specialize the results to either  $\rho^b$  or  $\rho^a$ ).

From Eq. 4 in the main text we have for diagonal and off-diagonal elements

$$i\dot{\rho}_{ii}(t) = \sum_j H_{ij}\rho_{ji}(t) - \rho_{ij}(t)H_{ji} \stackrel{t \rightarrow \infty}{=} 0 \quad (\text{S4a})$$

$$i\dot{\rho}_{ik}(t) = \sum_j H_{ij}\rho_{jk}(t) - \rho_{ij}(t)H_{jk} - i\tau_{deph}^{-1}\rho_{ik} \stackrel{t \rightarrow \infty}{=} H_{ik}(\rho_{kk}(t) - \rho_{ii}(t)) \quad (\text{S4b})$$

The first equation simply indicates that populations reach a stationary limit, while the second one has to be considered more carefully. Since  $\lim_{t \rightarrow \infty} \rho_{ik}(t) = 0$  also its derivative must go to zero and therefore

$$H_{ik}(\rho_{kk}(\infty) - \rho_{ii}(\infty)) = 0 \quad (\text{S5})$$

In the diabatic basis set Eq S5 implies that whenever  $H_{ik} \neq 0$  one has  $\rho_{kk}^b(\infty) = \rho_{ii}^b(\infty)$  i.e. in the stationary limit  $t \rightarrow \infty$  coupled diabatic states become equally populated (of course, if the initial state is not coupled either to  $|i\rangle$  or  $|k\rangle$  these states remain unpopulated). On the contrary, since in the adiabatic basis sets  $H_{ik} = 0$ , Eq. S5 is automatically fulfilled and therefore the populations of

different eigenstates are not bound to be equal. Trivially each adiabatic state conserves its initial population. Actually, Eq. S1a is fulfilled even at  $t=0$  so that, as it should be, at any time the populations are equal to their initial value  $\rho_{\mu\mu}^a(t) = \rho_{\mu\mu}^a(0)$ . Therefore, since in the long time limit  $\rho_{\mu\nu}^a(\infty) = 0$  we get  $\mathbf{\rho}^a(\infty) = \text{diag}(\rho_{\mu\mu}^a(0))$ ,  $\mu = 1, N$  and

$$\mathbf{\rho}^b(\infty) = \mathbf{C}\mathbf{\rho}^a(0)\mathbf{C}^T \quad \rho_{ii}^b(\infty) = \sum C_{i\mu}^2 \rho_{\mu\mu}^a(0) \quad (\text{S6}).$$

In Figure S5 the results of the dynamics with a dephasing  $\tau_{deph}^b = 100$  fs are shown. As we proved above, the diabatic populations are bound to reach a stationary-state where they are all equal, and this happens in a short-time for  $\tau_{deph}^b = 100$  fs. Since the ratio between the number of CT and Exc states increases as  $n-1$  at the increase of  $n$ , the number of units in the oligomer, this automatically causes a steep increase of the CT population at the increase of  $n$ . Such phenomenon is probably unphysical and introduce a too strong bias in our simulations.

#### S1.4. Changing the values of $t_h$ and $t_e$ parameters

It should be highlighted that changing the relative sign of  $t_h$  and  $t_e$  parameters can have a dramatic impact on the dynamics, while the effect of small differences in their absolute values is much more moderate. This is shown in detail in Figure S2 that compares the predictions of the electronic Hamiltonian for the two set of parameters  $t_h = 80 \text{ cm}^{-1}$  and  $t_e = 100 \text{ cm}^{-1}$  (exhibiting the same ratio of the values computed in ref. 66) and  $t_h = -100 \text{ cm}^{-1}$  and  $t_e = 100 \text{ cm}^{-1}$ . While in the former case the results are very similar to the ones reported in Figure 2, for  $t_h = -100 \text{ cm}^{-1}$  and  $t_e = 100 \text{ cm}^{-1}$  the extent of population transfer to CT states is strongly reduced. This is trivially due to the fact that, with this combination of signs, CT states only couple to the anti-symmetric combination of the Exc states, that is weakly absorbing, and gives therefore little contribution to the initial doorway state. However, the fact that  $t_h$  and  $t_e$  have the same sign can be considered assessed since: (i) this is what is computed in ref. 60 of the main text; (ii) Figure S2 indicate that the quality of the simulated absorption spectra deteriorates sensibly if  $t_h$  and  $t_e$  are given opposite signs, especially if, as in the simpler formulation of our Hamiltonian,  $t_{exc} = 0$ ; (iii) for  $t_h = -100 \text{ cm}^{-1}$  and  $t_e = 100 \text{ cm}^{-1}$ , the CT states exhibit a vanishing oscillator strength for  $W = 1200 \text{ cm}^{-1}$  (a value consistent with the most refined QM calculations in solution). On the other hand, ab initio calculations show that adiabatic states with dominant CT character bring a non-negligible oscillator strength, comparable with that of weak excitons, (see Improta & Barone *Angew. Chem., Int. Ed. Engl.*, 2011, 50, 12016-12019 and Lange & Herbert *J. Am. Chem. Soc.* 2009, 131, 3913-3922. ) and this can only be explained by a coupling with the symmetric (strongly absorbing) combination of the Exc states.

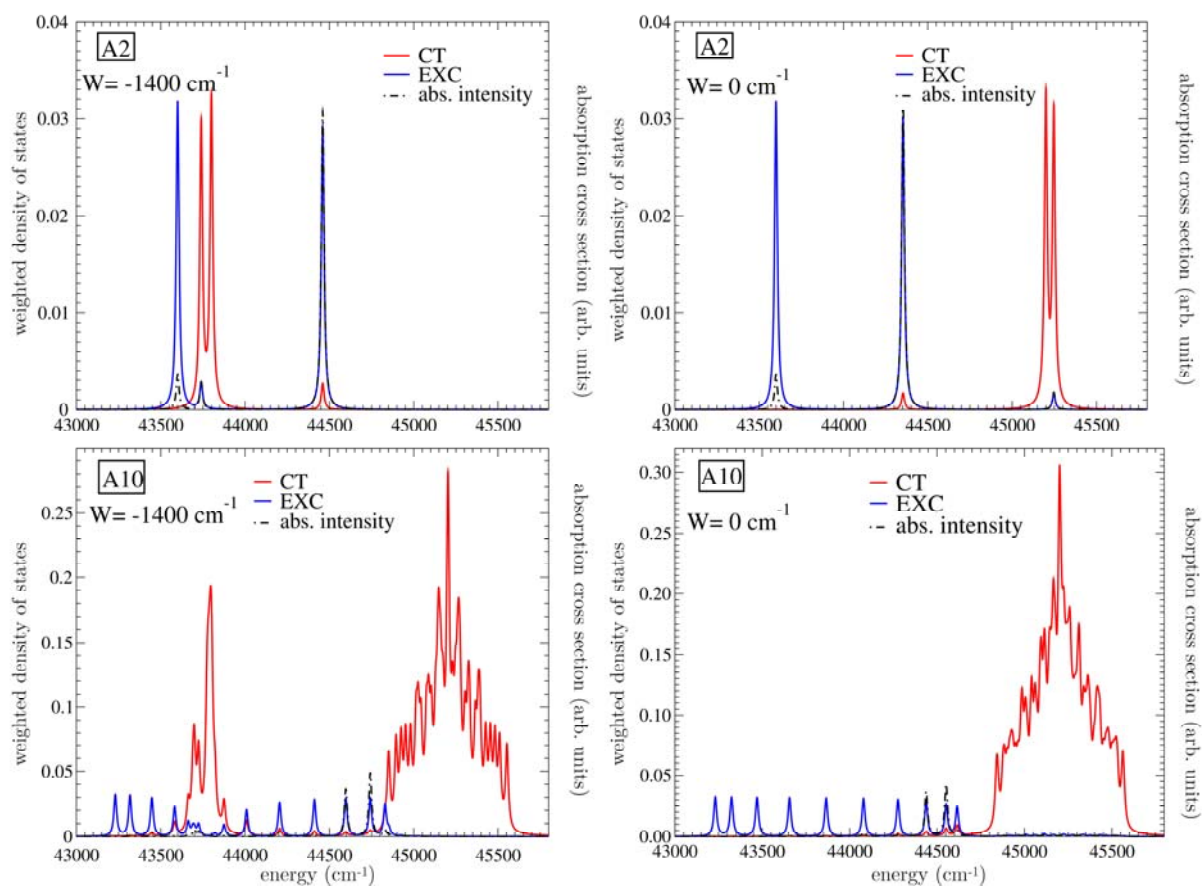


**Figure S1.** Plot of the weighted density of states for A<sub>10</sub> and W=-1400 (top panel), 0 (bottom panel) cm<sup>-1</sup>. A lorentzian broadening with  $\gamma=10$  cm<sup>-1</sup> is adopted. The integral over the frequency give the total number of CT (90) and Exc (10) diabatic states in the model. The absorption spectrum (in arb units) with same broadening is included for comparison.

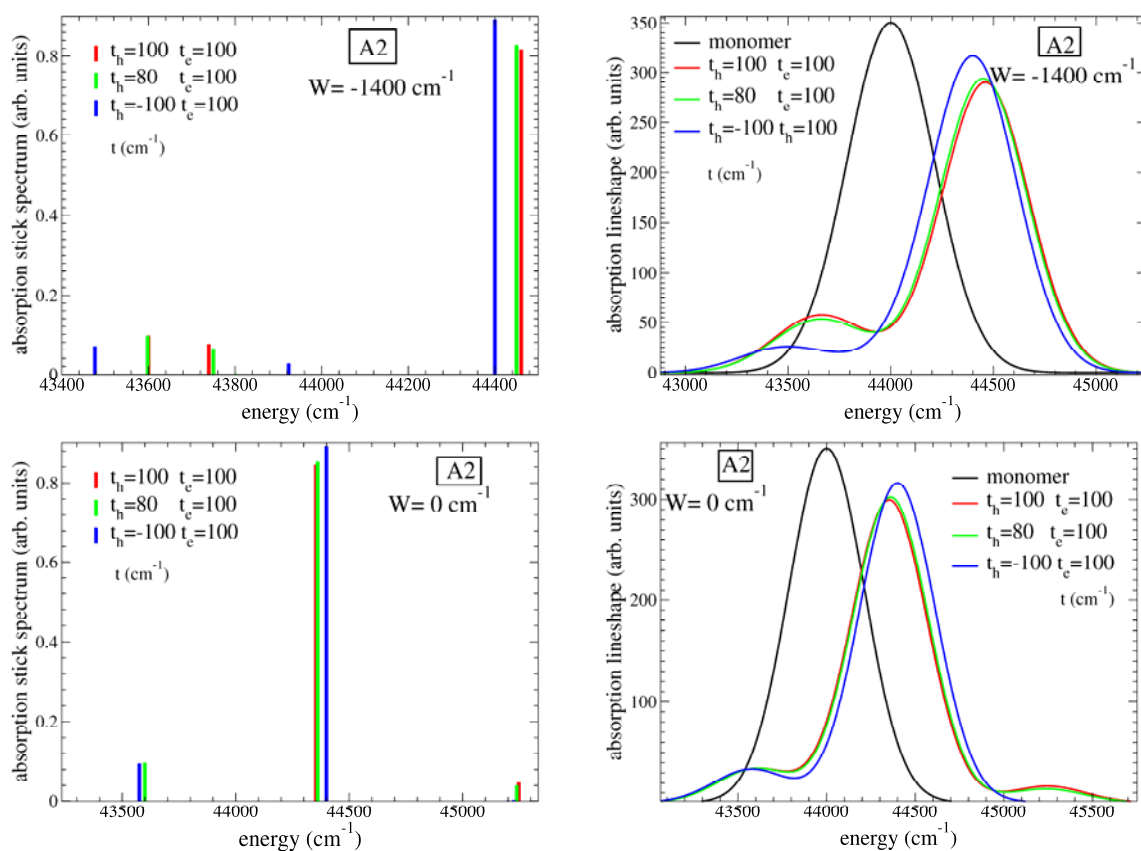


**Figure S2.** Stick (left panels) and convoluted (right panels) spectra, with a Gaussian with FWHM=500 cm<sup>-1</sup> obtained for the A<sub>2</sub> and A<sub>10</sub> systems and for the cases where CT states are more stable ( $W=-200$  cm<sup>-1</sup>, top panels) or less stable ( $W=1200$  cm<sup>-1</sup>, bottom panels). The results with the choice of the parameters  $t_h=t_e=100$  cm<sup>-1</sup> adopted in the main text are compared with those obtained with the different choices  $t_h=80$  cm<sup>-1</sup>,  $t_e=100$  cm<sup>-1</sup> and  $t_h=-100$  cm<sup>-1</sup>,  $t_e=100$  cm<sup>-1</sup>.

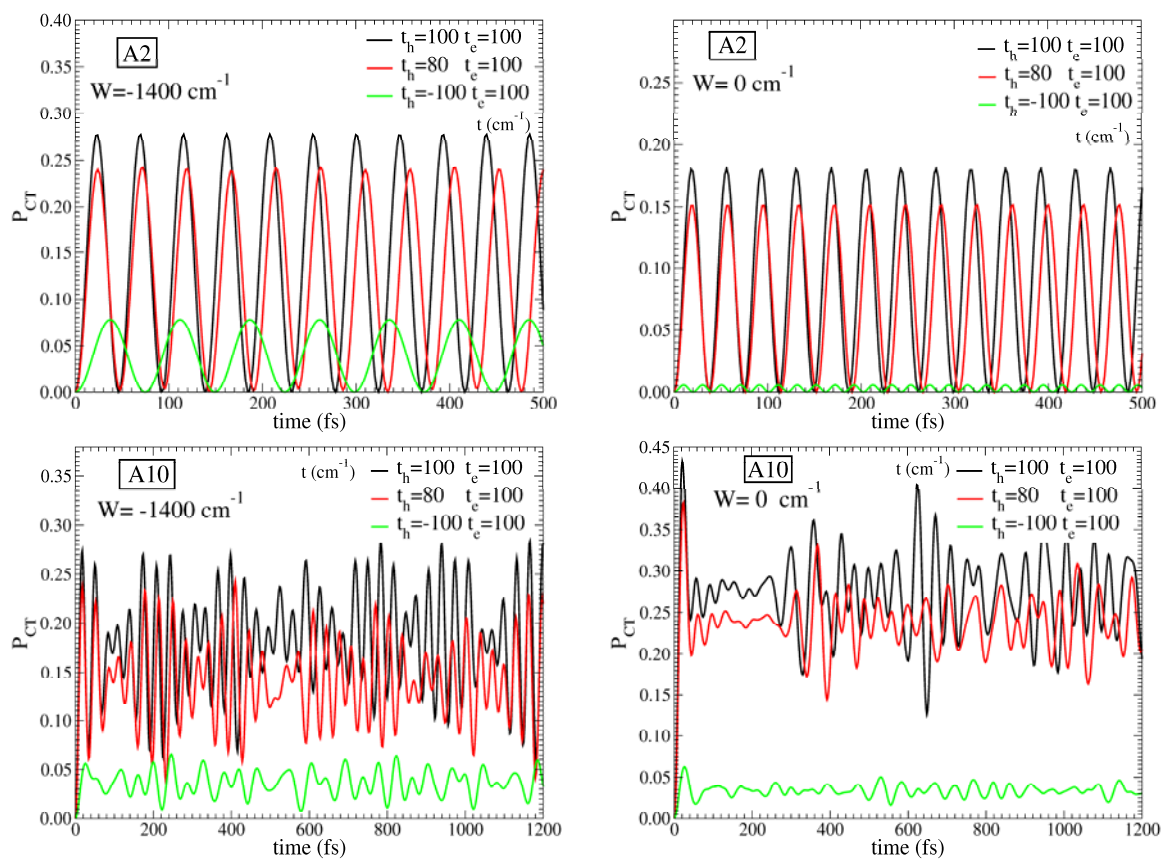


**Figure S3.** Time evolution of the diabatic CT population for  $A_2$  (top) and  $A_{10}$  (bottom) systems and for the cases where CT states are more stable ( $W=-14000\text{ cm}^{-1}$ , left panels) or less stable ( $W=0\text{ cm}^{-1}$ , right panels). The results with the choice of the parameters  $t_h=t_e=100\text{ cm}^{-1}$  adopted in the main text are compared with those obtained with the different choices  $t_h=80\text{ cm}^{-1}$ ,  $t_e=100\text{ cm}^{-1}$  and  $t_h=-100\text{ cm}^{-1}$ ,  $t_e=100\text{ cm}^{-1}$ .

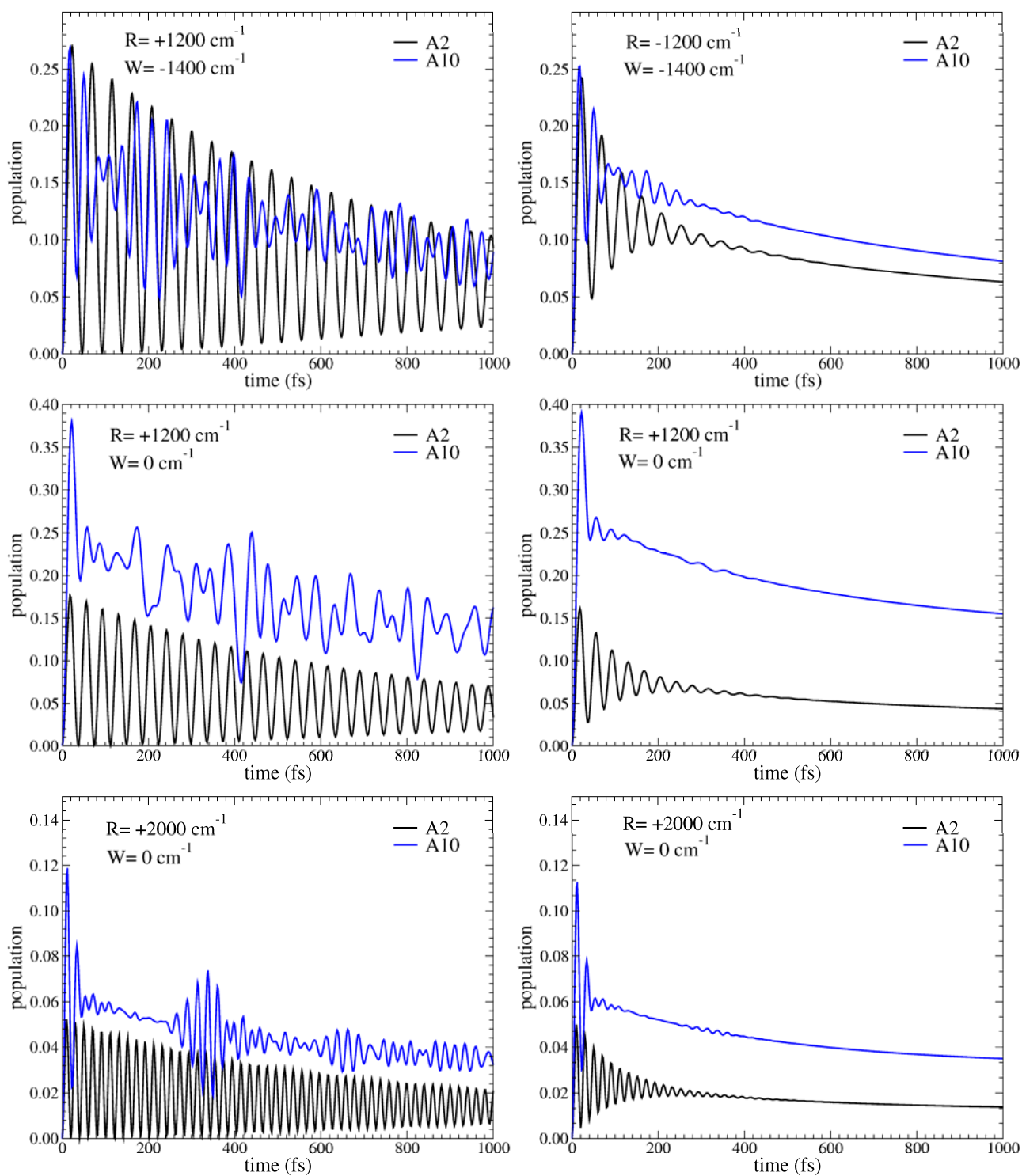


**Figure S4.** CT populations in  $A_2$  and  $A_{10}$  for three cases:  $W=-1400 \text{ cm}^{-1}$ ,  $R=1200 \text{ cm}^{-1}$ ;  $W=0 \text{ cm}^{-1}$ ,  $R=1200 \text{ cm}^{-1}$ ;  $W=0 \text{ cm}^{-1}$ ,  $R=2000 \text{ cm}^{-1}$  and two different choices of the dephasing time:  $\tau_{deph}^a = \infty$  (left panels),  $\tau_{deph}^a = 100 \text{ fs}$  (right panels).

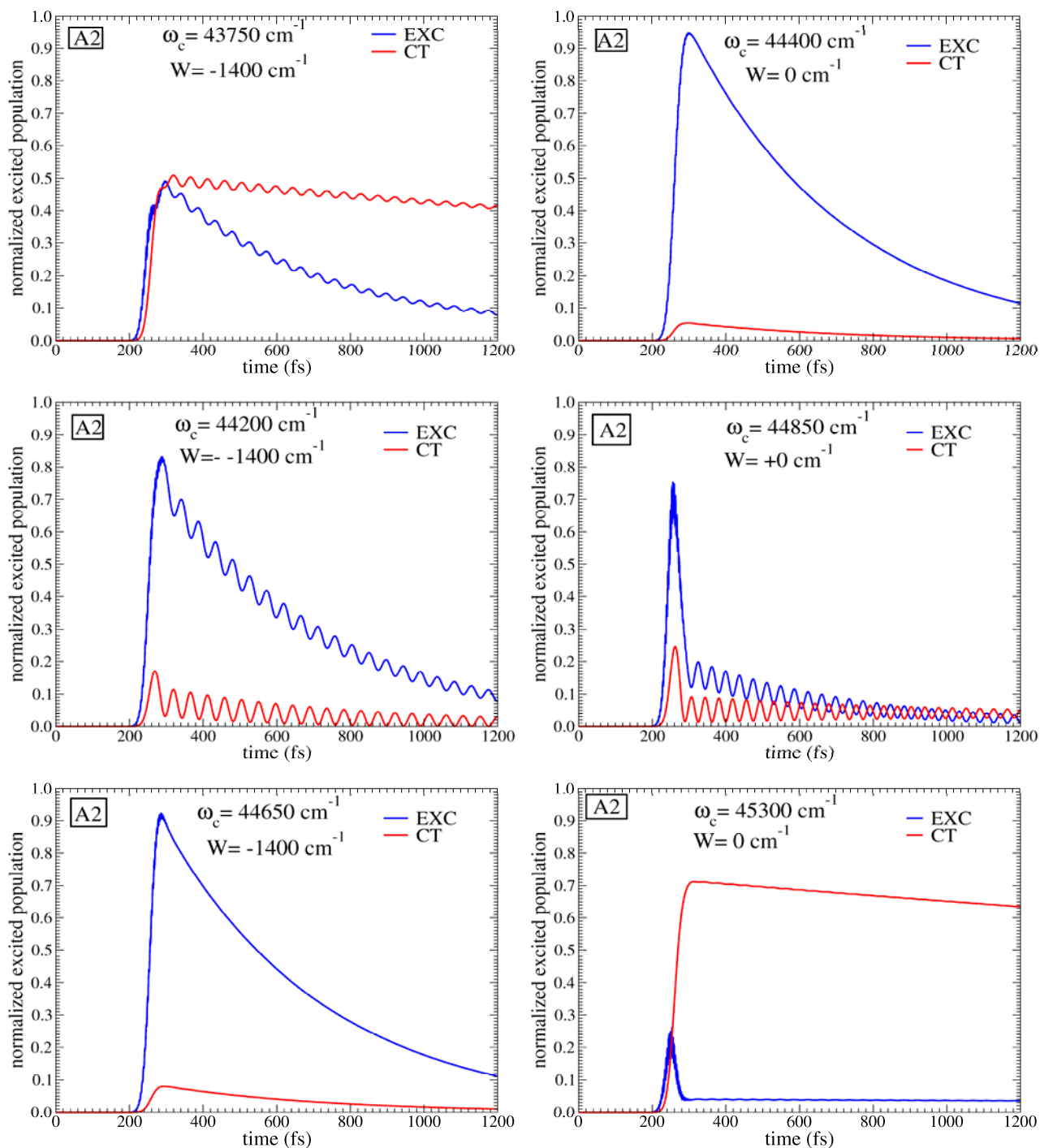


**Figure S5.** Time evolution of the diabatic CT and Exc populations for A<sub>2</sub> oligomer ( $\tau_{deph}^a = \infty$ , left panels:  $W = -1400$  cm<sup>-1</sup>, right panels  $W = 0$  cm<sup>-1</sup>) excited by a laser pulse with FWHM=50 fs, central time  $t_0 = 250$  fs and different carrier frequencies  $\omega_c$  indicated in the panels and roughly in resonance with the frequencies of the two maxima of the absorption spectra in Figure 1 and their average. The excited population  $P_{EXC}(t) + P_{CT}(t)$  is normalized to 1 at its first maximum (always falling at  $\sim 280$  fs). The absolute population excited is actually strongly dependent on  $\omega_c$  being respectively 0.32, 0.73, 1 for  $\omega_c = 43750, 44200$  and  $44650$  cm<sup>-1</sup> ( $W = -14000$  cm<sup>-1</sup>) and 1, 0.11, 0.08 for  $\omega_c = 44400, 44850$  and  $45300$  cm<sup>-1</sup> ( $W = 0$  cm<sup>-1</sup>).